Urban Forestry & Urban Greening 13 (2014) 785–792

Contents lists available at ScienceDirect

Urban Forestry & Urban Greening

journal homepage: www.elsevier.com/locate/ufug

Modeling of urban trees' effects on reducing human exposure to UV radiation in Seoul, Korea

Hang Ryeol Na[a,*], Gordon M. Heisler[b], David J. Nowak[b], Richard H. Grant[c]

[a] Department of Science, Technology and Society/Public Policy, Rochester Institute of Technology, 1313 Eastman, Rochester Institute of Technology, 1 Lomb Memorial Drive, Rochester, NY 14623, United States
[b] USDA Forest Service, Northern Research Station, 5 Moon Library, SUNY-ESF, Syracuse, NY 13215, United States
[c] Department of Agronomy, Purdue University, Life Science Plant and Soil, Room 215, United States

ARTICLE INFO

Keywords:
Human health
i-Tree
Ultraviolet (UV)
Urban forestry
UV protection factors (UPF)

ABSTRACT

A mathematical model is constructed for quantifying urban trees' effects on mitigating the intensity of ultraviolet (UV) radiation on the ground within different land use types across a city. The model is based upon local field data, meteorological data and equations designed to predict the reduced UV fraction due to trees at the ground level. Trees in Seoul, Korea (2010), produced average UV protection factors (UPF) for pedestrians in tree shade at solar noon (May to August) of 8.3 for park and cemetery land uses and 3.0 for commercial and transportation land uses. The highest daily UPF was 11.8 in the park and cemetery land uses, which has the highest percent canopy cover. This UV model is being implemented within the i-Tree modeling system to allow cities across the world to estimate tree effects on UV exposure. Understanding the impacts of urban trees on UV exposure can be used in developing landscape design strategies to help protect urban populations from UV exposure and consequent health impacts.

Introduction

Ultraviolet (UV) radiation, part of the electromagnetic spectrum emitted by the sun, is classified as a human carcinogen (e.g., skin cancer), according to the World Health Organization (WHO) (IARC, 2012) and the U.S. Department of Health and Human Services (NTP, 2011). Prolonged exposure to UV radiation can also cause adverse health effects on eyes and the immune system, although a small amount of it is beneficial in the production of vitamin D (e.g. Lucas, 2010). Hence, government policies for sun safety include 'seek shade when possible' (US EPA, 2010; WHO, 2002) and 'plant trees' for protection from UV radiation (US HHS, 2012).

It is well documented in the literature that trees, including the scattered individual trees in urban settings, reduce UV radiation in their vicinity. For example, Heisler and Grant (2000) empirically showed that urban tree shade greatly reduces UV irradiance when they obscure both the sun and sky view. In small sunny areas, where nearby trees that block much of the sky from view, UVB (280–315 nm) irradiance is reduced substantially, whereas visible irradiance may be nearly as great or slightly greater than that in the open (Heisler et al., 2002). Thus, it is possible to protect the human population from harmful UV radiation through urban landscape designs that include trees and other vegetation (Yoshimura et al., 2010).

Other studies have also quantified UV radiation reduction provided by trees. Yang et al. (1993) measured the vertical profiles of foliage area and solar irradiance in the UVB, photosynthetically active (PAR, 400–700 nm), and total spectral (broadband or whole spectrum radiation) regions in a partially defoliated mixed oak forest, and showed that the attenuation rate was greatest for UVB, smallest for the total spectral region and intermediate for PAR. Diffey and Diffey (2002) found that UV protection factors (UPFs), conceptually equivalent to the sun protection factor (SPF) used to indicate sunscreen protection levels, for single trees ranged from 4 to 20 and that venturing into even a small wooded area could increase the UPF up to 100, which is similar to the findings of Yang et al. (1993). Parsons et al. (1998) found UPFs of summer midday tree shade ranged from 3.5 to 5.5, while Parisi and Kimlin (1999), who did spectral measurements in tree shade of five typical Australian trees, found UVB and erythemal UV shade ratios of 0.15–0.35, giving equivalent UPFs of 3–6. Gies et al. (2007) concluded that the measured UPFs ranged from 5 to 10 and were generally a maximum in the height of summer when the sun was highest in the sky and the foliage was densest. Erythema is a medical term for redness or inflammation of the skin produced by congestion of the capillaries in the skin.

* Corresponding author. Tel.: +1 6462450579.
E-mail address: nhr24@hotmail.com (H.R. Na).

http://dx.doi.org/10.1016/j.ufug.2014.05.009
1618-8667/

Table 1
Whole leaf reflectance, transmittance and absorbance to UV radiation (300 nm) of tree species that are found growing in Seoul.

Species	Reflectance[a]	Transmittance[a]	Absorbance[a]
Liriodendron tulipifera	4.807	0.0002	95.191
Platanus occidentalis	6.824	0.012	93.164
Populus deltoides	7.337	0.001	92.662
Pyrus calleryana	6.088	0.002	93.91
Quercus acutissima	6.634	0.167	93.199
Quercus palustris	5.843	0.005	94.152

[a] Source: Qi et al. (2010), values are in percentages (%).

Studies about spectral absorbance, reflectance and transmittance of tree leaves to UV radiation (e.g. Yang et al., 1995; Grant et al., 2003; Qi et al., 2010) generally conclude that about 90–95% of UV is absorbed, 5–9% reflected and <0.1% transmitted through leaves regardless of tree species. Leaf characteristics in relation to UV radiation of select tree species that are found in Seoul are given in Table 1.

Models of UV irradiances in tree shade have been created to represent erythemally effective UV radiation exposure within a school environment (Downs et al., 2008) and for predicting relative irradiance beneath tree canopies for both UVB and PAR on the horizontal level under clear skies (Heisler et al., 2003a,b). Grant et al. (2002) also developed a model to predict UVB irradiance in fields in open-tree canopies under clear skies. They concluded that UPFs were generally less than 2 for areas with less than 50% canopy cover and that UPFs of 10 were possible at all latitudes for 90% canopy cover. These models have limitations related to environmental settings (e.g. school) or weather conditions (clear or cloudy sky). Consequently, Grant and Heisler (2006) produced multivariate regression equations to overcome these limitations by considering the full range of sky conditions for the entire area of Baltimore, MD.

The purpose of this study is to model urban trees' effects on reducing UV radiation in Seoul, Korea by employing the multivariate equations from Grant and Heisler (2006) and to estimate a protection factor in different land uses on a city-wide scale. This study incorporates local field data collected in Seoul and analyzed using the i-Tree model (Nowak et al., 2008) with local UV and cloud data to estimate the impact of trees in Seoul on reducing UV radiation exposure to humans.

Methods

To estimate tree effects on reducing UV irradiance, four data sets for Seoul were required: (1) canopy cover; (2) UV index; (3) hourly cloud cover; and (4) solar zenith angle data. These data were then combined with equations (Grant et al., 2002; Heisler et al., 2003a,b; Grant and Heisler, 2006) to predict the reduction in the UV protection factors due to trees within each city land use for mid-day conditions for the period of May 1 to August 31, 2010.

Canopy cover data

Field data on vegetation in Seoul, Korea was collected in the summer of 2010 based on random sampling of two hundred 0.04-ha circular plots throughout the city area. These data were entered into the i-Tree Eco model (Nowak et al., 2008) for analysis of structural characteristics and several ecosystem services and values (www.itreetools.org) as part of another project to estimate ecosystem services. In each field plot, tree, shrub and ground cover types and percentages were estimated to categories of five percent for a reasonable degree of accuracy. As will be shown in the Results section, a part of the i-Tree analysis result includes percent canopy cover according to different land use types. Estimates were derived for 6 different land use types: commercial/transportation, institutional, residential, park/cemetery, vacant/agriculture and water. Vacant land included land with no clear use or ownership and was often in forested mountainous areas.

Although canopy cover may increase during summer, the possible temporal change in canopy cover is not precisely considered in this project. The reason is that the field data was being measured and collected throughout the four months from May to August in 2010 in 200 sample plots across the entire city of Seoul, which is larger than 605 km^2.

Table 2
Relevant parameters for computing UVI and a rough estimate of the introduced uncertainty in a practical forecast.

Parameter	Uncertainty in UVI (%)
Cloud amount and properties	>50
Albedo (snow)	28
Ozone profile	8
Aerosol properties ($\tau = 0.42 \pm 0.26$)	5
Altitude (1 km)	5
Total ozone (3%)	4
Geographical latitude (1°)	3
Distance from Sun to Earth	3
Stratospheric temperature (10°)	2
Sulphur dioxide (1 DU)	1

Source: Allaart et al. (2004)

UV Index

UV index (UVI) data were obtained from the project Tropospheric Emission Monitoring Internet Service (TEMIS; http://www.temis.nl/uvradiation/), which provides near-real time data on total ozone and surface UV data (van Geffen et al., 2005). UV data are based on SCIAMACHY (SCanning Imaging Absorption spectroMeter for Atmospheric CHartographY) observations. SCIAMACHY is a passive remote sensing spectrometer observing backscattered, reflected, transmitted or emitted radiation from the atmosphere and Earth's surface, in the wavelength range between 240 and 2380 nm on board ENVISAT satellite (SCIAMACHY, 2012).

As a global standard measurement of the strength of UV radiation from the sun at a particular place on a particular day, the unitless UVI is defined as (e.g. WHO, 2002):

$$\mathrm{UVI} = \frac{40}{Wm^2} \int_{250\ \mathrm{nm}}^{400\ \mathrm{nm}} E_\lambda S_{er}(\lambda) d\lambda \quad (1)$$

where $E(\lambda)$ is the solar spectral irradiance expressed in $W/(m^2\ nm)$ at wavelength λ and $d\lambda$ is the wavelength interval used in the summation. $S_{er}(\lambda)$ is the International Commission on Illumination (CIE) reference action spectrum for UV-induced erythema on the human skin (McKinlay and Diffey, 1987; CIE, 1987). Although there is no input of cloud cover to Eq. (1), it is recommended that UVI forecasts should include effects of cloud cover on UV radiation transmission through the atmosphere. When cloud effects are not incorporated in the forecasts, the UVI should be referred to as a 'clear sky' or 'cloud free' UVI (WHO, 2002, p. 6). Clouds can substantially reduce UV and visible solar radiation (Fioletov et al., 2010). Table 2 lists the factors influencing the UVI with their uncertainty weight.

The UVI data from TEMIS is a clear sky UVI, expressed as a function of solar zenith angle (SZA, angle of the sun from directly overhead) and total ozone, which gives relatively good results for all SZAs between 0° and 90° and a wide range of total ozone values (Allaart et al., 2004). As it does not take into account sky conditions, we adjusted the UVI according to the local cloud data.

There are several different methods of accounting for cloud cover in calculating the UVI. For example, Vanicek et al. (1999) provided a table of Cloud Modification Factors (CMF), assigning numbers between 0 and 1, for different cloud types at different

Table 3
Percent UV radiation transmission rates according to sky conditions.

Sky condition[a]	Transmission rate (%)
CLR and FEW	99.9
SCT	89.6
BKN	72.6
OVC	31.6

Modified from Kinney et al. (2000) based on Grant and Heisler (2006).
[a] CLR (clear) means no clouds below 12 thousand feet. FEW means few (less than 1 tenth sky cover). SCT means scattered clouds (1 tenth to 5 tenths sky cover). BKN means broken clouds (6 tenths to 9 tenths sky cover). OVC means overcast (10 tenths sky cover). (NOAA description of weather observations at http://www.erh.noaa.gov/box/obshelp.htm).

altitudes. They also developed an equation to calculate the cloudy-sky UVI along with the CMF. Kinney et al. (2000) presented the percent radiation transmission rates according to sky conditions by using the MOS (Model Output Statistic) cloud probabilities. The transmission rates (Table 3) are used for the UVI calculation by the US Environmental Protection Agency (EPA) and the National Weather Service (US EPA, 2012). Following the definition of the WHO, the Korea Meteorological Administration does not take cloud into consideration when calculating the UVI forecast.

We used local cloud cover data to calculate the estimated UVI adjusted for cloud effects (Table 3) as:

$$UVI = UVI_0^{*}\,\text{transmission rate} \quad (2)$$

where UVI_0 is the UVI under clear sky conditions.

Seasonal average of *UVI* for Seoul from May 1 to August 31, 2010 was 5.80, whereas that of UVI_0 was 8.24, about 1.42 times higher than *UVI*. This difference matches well with Kim et al. (2011), who found that the values of TEMIS UVI under cloud-free conditions are 1.5 times higher than the all-sky measurements by a Brewer Spectrophotometer for the period 2004–2010 in Seoul.

This study used UVI rather than erythemally weighted UV (in W/m^2) because UVI is a means of informing the public about the strength of biologically effective, erythemally weighted UV radiation. The World Health Organisation (WHO) and the World Meteorological Organisation (WMO) have jointly recommended that the UVI should be used to inform the public about possible health risks due to overexposure to solar radiation, especially skin damage (de Backer et al., 2001). Since its introduction in Canada in 1992, the UVI has become a widely used parameter to characterize solar UV radiation (Fioletov et al., 2010).

Cloud cover

Cloud cover is a necessary factor affecting human exposure to UV radiation. Grant and Heisler (2006) concluded that lack of cloud cover data in estimating erythemal exposure for people in Baltimore resulted in a 40% overestimate of protection across the entire under-canopy space and 20% overestimate of protection in the shaded areas of the canopy. This result was despite the fact that the erythemal UV irradiance under skies with 50% or less cloud cover was not remarkably different from that under clear skies. In tree shade, the actual irradiance was greater under partly cloudy than under clear skies (Grant and Heisler, 2006).

This insignificant effect on irradiance of small amounts of cloud cover might be because the attenuation by clouds depends on both the thickness and the type of clouds (optical depth of clouds). Thin or scattered clouds have only a small effect on UV at the ground level. Under certain conditions and for relatively short periods, a small amount of cloud cover may even enhance the UV irradiance compared to fully clear skies (Vanicek et al., 1999) due to UV radiation reflection from clouds (WHO, 2002). In general though, clouds can substantially reduce UV and visible solar radiation. In the UVA range 315–400 nm, irradiance can be reduced by a factor of more than 100 under heavy thunderstorm clouds compared with that of clear sky conditions, and the reduction can be even stronger in UVB (Fioletov et al., 2010).

Cloud cover data were obtained for noon of each day. As the available sky condition data are 3-h interval data, noon was the closest time to the local time of solar noon. The cloud data were obtained from the Integrated Surface Database (ISD) provided by the National Climatic Data Center (NCDC) of US National Oceanic and Atmospheric Administration (NOAA) at http://www.ncdc.noaa.gov/oa/climate/isd/index.php.

Solar zenith angle

Solar zenith angle is also necessary to model irradiance because the intensity of solar UV, especially UVB, depends on the elevation of the sun in the sky. For small SZA's, the UV radiation is more intense because the rays from the sun have a shorter path through the atmosphere and therefore have less atmospheric absorption. The SZA changes with latitude, season, and time of day (Vanicek et al., 1999). UV intensities are usually highest during the summer months in the 4-h period around solar noon. UVB intensity varies more with the time of the day than does UVA (WHO, 1995). In this case study of Seoul, SZA at solar noon ranges from 13.9 degrees (0.24 radians) on June 21 to 28.6 degrees (0.5 radians) on August 31.

This study models tree effects at solar noon of each day during the study period, approximately the time when the sun is highest above the horizon. This time was selected to match the time used in the UV index. Korean local time of solar noon from May 1 to August 31 of 2010 was 12:30 pm ± 5 min (http://www.solar-noon.com). The local SZA for Seoul was computed for 12:30 pm of each day in our study period by the Measurement and Instrumentation Data Center (MIDC)'s SOLPOS (Solar Position and Intensity) calculator provided by the US National Renewable Energy Laboratory (http://www.nrel.gov/midc/solpos/solpos.html).

Modeling reduction in UV Irradiance

The percent of UV irradiance received below the tree canopy (T_s) depends, in part, on sky conditions relative to the above-canopy clear sky irradiance. T_s was calculated from multivariate regression equations based on an 11 × 11 array of trees (Fig. 1) for various SZA's (Grant et al., 2002). The equations were run for each land use with the size of opaque ellipsoidal tree crowns in the 11 × 11 array adjusted according to percent of canopy cover in each land use as determined by the field data (i.e., tree sizes will increase as canopy cover increases). The 11 × 11 array is a virtual setting for computing the value of T_s, whereas the sample plot of 0.04 ha circular size is a physical boundary for collecting plot data. Thus, the size of a sample plot cannot affect the virtual array.

A pedestrian would experience a different value of T_s depending on whether he or she was in a shaded area or not. 'Shaded' area refers to the areas in the shadow of direct beam PAR, as they would appear to human eyes (Fig. 1). The shaded fraction and sunlit fraction of T_s were determined for the region under the four central crowns in the 11 × 11 array to minimize edge effects. The values of T_s were then regressed against solar zenith angle and canopy cover fraction to provide a means to relate below-canopy irradiance to above-canopy irradiance for locations with given latitudes on given days and times (Grant and Heisler, 2006). For average in-shade below canopy locations:

$$T_s(C, \theta, m, \text{shaded}) = (a + b\theta^c)(1 - m) - (\theta^d/e)\sin(\pi m) \quad (3)$$

where C = cloud cover, θ = SZA in radians, m = canopy cover, and a, b, c, d, e are coefficients for predictions (Table 4).

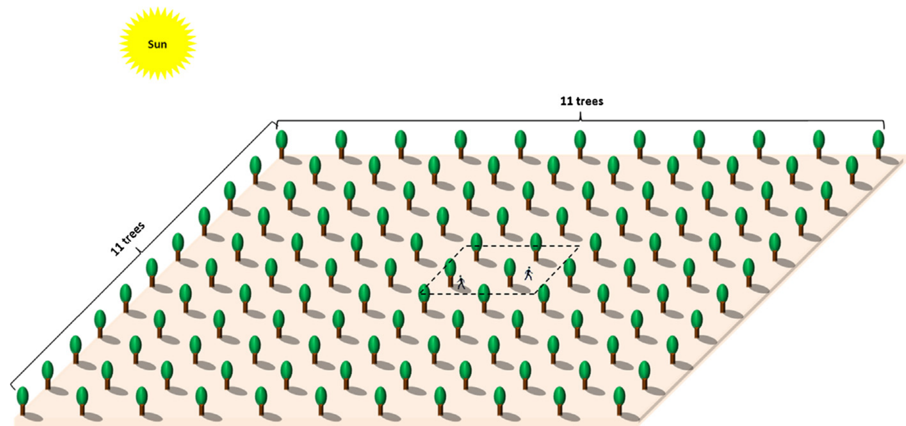

Fig. 1. The measured cover fraction was represented by a regularly distributed 11 × 11 array of spherical tree crowns.

Table 4
Coefficients for prediction of UV exposure in average in-shade locations (Eq. (3)).

Cloud cover[a] (*C*)	*a*	*b*	*c*	*d*	*e*
CLR and FEW	0.261	0.407	1.5	0.969	7.24
SCT	0.315	0.527	2.97	1.79	5.72
BKN	0.259	0.37	2.63	1.82	7.78
OVC	0.06	0.316	0.97	1.86	13.63

Source: Grant and Heisler (2006)
[a] Sky condition definitions in Table 3.

Table 5
Coefficients for prediction of overall UV exposure (Eq. (4)).

Cloud cover[a] (*C*)	*A*	*b*	*c*
CLR and FEW	1	0.598	4.77
FEW	1	0.598	4.77
SCT	0.931	0.447	5.02
BKN	0.683	0.252	7
OVC	0.368	0	14.87

Source: Grant and Heisler (2006)
[a] Sky condition definitions in Table 3.

As pedestrians do not stay in shade all the time, mean spatial overall exposure (both sun and shade exposure) across the entire array for varying cloud cover is calculated as:

$$T_s(C, \theta, m, \text{all}) = a(1 - m) - (\theta^b/c)\sin(\pi m) \quad (4)$$

based on variables given in Table 3. Eqs. (3) and (4) were fit to predictions of relative irradiance that were modeled by the UV radiation transfer (UVRT) model (Grant and Heisler, 2006; Table 5).

Trees were evenly arranged in the model based on the assumption that a sky radiance of UV is isotropically distributed in a given land use. The uniform arrangement of trees is based on empirical observations that the diffuse fraction of UV irradiance is largely determined by the sky view factor (e.g. Heisler et al., 2003a,b). However, it was an assumption simplifying the actual tree arrangements. We multiplied *UVI* by T_s to estimate the reduction in *UVI* due to trees within each land-use category.

UV protection factor

Following the previous studies such as Grant et al. (2002), Diffey and Diffey (2002) and Gies et al. (2007), UV protection factor (UPF) is the ratio of mean irradiance in direct, unshaded sunlight to that in tree shade. The unshaded value in our case is the *UVI* value calibrated according to sky conditions, and the under-tree shade value is *UVI* multiplied by T_s, which becomes a fraction of the *UVI* below the tree canopy.

UPF is conceptually equivalent to the sun protection factor (SPF) used to indicate sunscreen protection, given the basic definition of SPF (e.g. Bleasel and Aldous, 2008) as the ratio of the Minimal Erythema Dose (MED) on product protected skin to the MED on unprotected skin. MED is a measure of the amount of energy per unit area ($\mathrm{J\,cm^{-2}}$) required to cause minimal erythema on light-skinned individuals. Likewise, the UPF of urban trees can be defined as how many times longer a person would have to spend in a particular environment to receive the same exposure as in an open location with no solar UV protection (Grant and Heisler, 2006). Fig. 2 illustrates the process of calculating a daily UPF value for pedestrians in tree shade.

Results

According to the i-Tree analysis based on the field data from Seoul, the urban forest of Seoul has an estimated 18,865,000 trees with canopies that cover 31.1 percent of the area (Table 6). Canopy cover was highest in park/cemetery land uses and lowest in water. This varying cover had differing effects on reducing human exposure to UV radiation.

Monthly UPF

As expected, the greater the canopy cover, the greater the UPF (Tables 7 and 8). However, the relationship between canopy cover and UPF is not directly proportional. For example, canopy cover of urban trees in park/cemetery land use is more than five times that of commercial/transportation land use, whereas the UPF value of park/cemetery, 8.3, is less than three times that of commercial/transportation, 3.0. Protection factors were greatest in park/cemetery land uses and lowest in commercial/transportation land uses.

The overall UPF for the entire city for all months was estimated to be 4.1. In other words, the seasonal average of *UVI* for Seoul, 5.8 was reduced to 1.4 by tree shade. This result conforms with the previous study of Baltimore, in which the UPF was 4.5 for shaded areas (Grant and Heisler, 2006). The *UVI* reduction by more than 4 can be considered as significant, given that protection is necessary above the threshold value of *UVI* 3 (WHO, 2002).

Comparison of Tables 7 and 8 indicates that a pedestrian in constant tree shade has more than double the UV protection than average overall exposure in the same land use type.

Daily UPF

Daily minimum and maximum values of UPF by land use illustrate that protection from trees varies daily based on

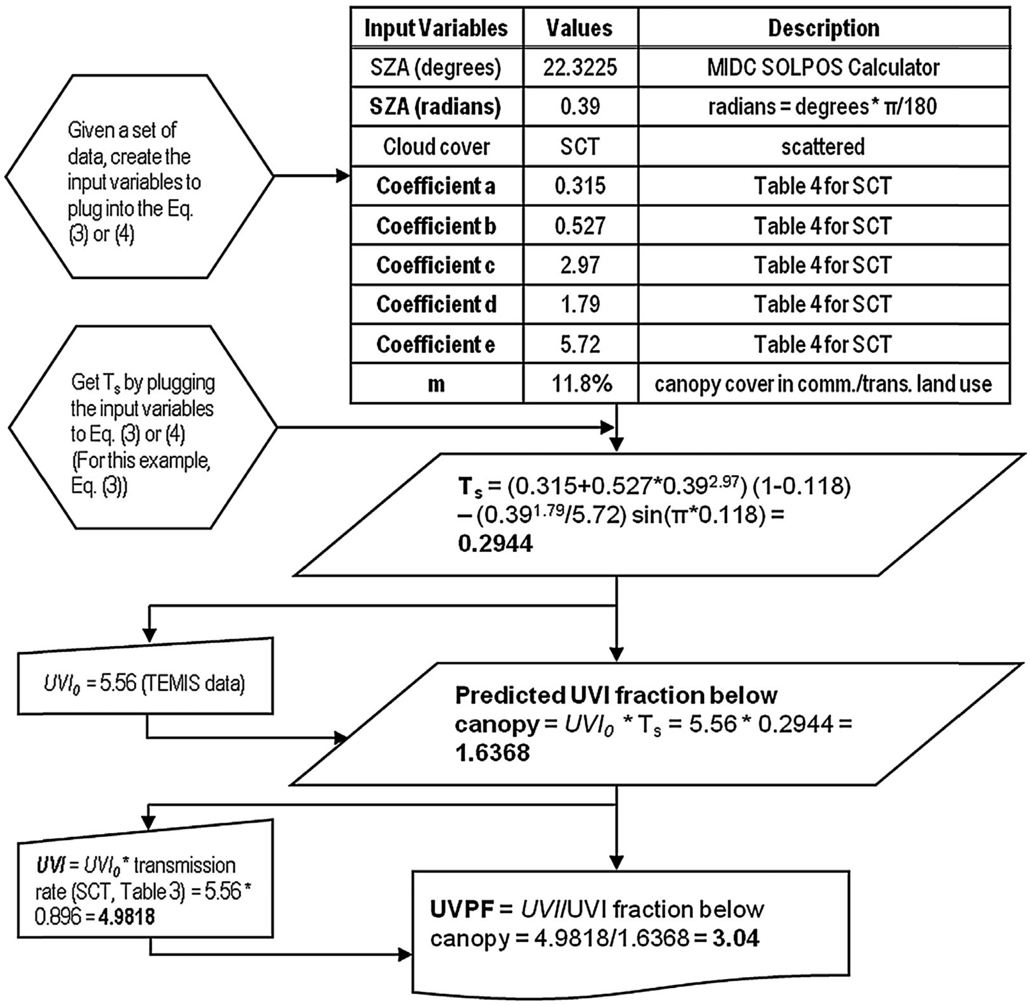

Fig. 2. Example modeling process of calculating a daily UV protection factor of urban trees in commercial and transportation land use type in Seoul on May 1, 2010.

meteorological conditions (Table 9). Maximum daily UPF was 11.8 in tree shade in park/cemetery areas; minimum daily UPF value was 1.1 for overall condition in commercial/transportation areas.

Differences in UPF, ΔPF, between the land use type with the highest percent canopy cover, park/cemetery, and that with the lowest canopy cover, commercial/transportation land use, range from 2.2 to 8.4 (Table 10). In tree shade, the greatest ΔPF, 8.4 occurred on August 17 when the cloud cover was clear, whereas the lowest ΔPF, 3.2 on August 31 with overcast sky condition and the greatest SZA.

Maximum daily UPF in tree shade was 11.8 in Park/cemetery on May 20, 2010, indicating that trees can have substantial impacts in helping protect human populations from UV exposure.

Table 6
Ground cover composition (percent coverages) in Seoul by land use.

Ground cover	Land use						City total
	Comm./trans.[a]	Institutional	Residential[b]	Vacant/ag.[c]	Park/cemetery	Water	
Building	25.6	14.8	34	4.4			16.3
Cement	17.8	18.1	12.5	0.5	2.3		10
Tar	33.5	2.7	28.8	1.6	7.6		16
Bare soil	9.6	31.6	6.8	31.4	22.7		17.9
Rock	6.8	12.5	9.2	2.2	6.8		7.2
Duff/Mulch		1.9		30.9	26.8		10.5
Herbs	0.8	3.8	4.1	19.5	11.4		7.1
Grass	4.7	5.4	3.5	1.9	6.3		4.2
Wild grass	1.2	5.2	0.9	8.6	5.8		3.8
Water		4	0.2	1.9	7.6	100	7
Total							100
Canopy cover	**11.8**	**14.9**	**19.2**	**60.2**	**62**		31.1

[a] Commercial/transportation.
[b] Residential includes a multi-family residential land use type.
[c] Vacant/Agriculture: The category 'Vacant' includes land with no clear intended use. In Seoul, it was often a mountainous area with no evident use or ownership. Similar to 'park' it had relatively many trees.

Table 7
Mean values of *UVI* below canopy and urban tree canopy UPF in each land use of Seoul for UV exposure in tree shade.

Month	Land use					UVI above canopy
	Comm./trans.	Institutional	Residential	Vacant/ag.	Park/cemetery	
Predicted UVI below canopy						
May	1.7	1.6	1.5	0.6	0.6	5.3
June	1.8	1.7	1.6	0.7	0.7	6.0
July	2.0	1.9	1.8	0.8	0.8	6.1
August	2.1	2.0	1.9	0.8	0.7	5.8
All months	1.9	1.8	1.7	0.7	0.7	5.8
UPF (UVI above canopy divided by Predicted UVI below canopy)						
May	3.1	3.2	3.5	8.3	8.8	
June	3.3	3.5	3.7	8.5	8.9	
July	3.0	3.2	3.4	7.6	7.9	
August	2.7	2.9	3.1	7.4	7.8	
All months	3.0	3.2	3.4	7.9	8.3	

Table 8
Mean values of urban trees' UPFs in each land use of Seoul for overall UV exposure.

Month	Land use Comm./trans.	Institutional	Residential	Vacant/ag.	Park/cemetery	UVI above canopy
Predicted UVI below canopy						
May	4.5	4.3	4.0	1.5	1.4	5.3
June	5.1	4.8	4.5	1.7	1.6	6.0
July	5.0	4.8	4.4	1.6	1.5	6.1
August	4.8	4.5	4.2	1.5	1.4	5.8
All months	4.9	4.6	4.3	1.6	1.5	5.8
UPF (UVI above canopy divided by predicted UVI below canopy)						
May	1.2	1.2	1.3	3.6	3.8	
June	1.2	1.2	1.3	3.5	3.7	
July	1.2	1.3	1.4	3.9	4.1	
August	1.2	1.3	1.4	4.0	4.2	
All months	1.2	1.3	1.4	3.8	4.1	

Table 9
Daily maximum and minimum of UPFs by land use.

Land use	Comm./trans.	Institutional	Residential	Vacant/ag.	Park/cemetery
In-shade UV protection					
Max.	3.8	4.0	4.3	11.1	11.8
Min.	1.7	1.8	1.9	4.6	4.8
Overall UV protection					
Max.	1.3	1.4	1.5	4.6	4.9
Min.	1.1	1.1	1.2	3.2	3.4

Table 10
ΔPF between the land uses with highest (park/cem.[a]) and lowest canopy cover (comm./trans.).

	In-shade UPF	Overall UPF
Maximum	8.4	3.6
Minimum	3.2	2.2
Monthly mean		
May	5.6	2.8
June	5.6	2.6
July	4.8	3.0
August	4.9	3.1
Seasonal mean (for all months)	5.2	2.9

[a] Cemetery.

Government policies recommend applying a sunscreen with a SPF of 15 or more for UVI of 6 or more (e.g. US EPA, 2010).

Cloud effect

The cloud cover was clear when the maximum UPF 11.8 was recorded. In contrast, the lowest UPF both in shade (1.7 on August 31) and overall (1.1 on May 24) exposures happened when the sky condition was overcast, which indicates that the influence of the cloud cover on the T_s (in the shaded areas) was greatest for overcast skies. This is in agreement with the suggestion of Grant and Heisler (2006) that the effectiveness of shade to reduce exposure to UVB irradiance is generally not dependent on the cloud except under overcast skies.

The greatest ΔPF in a clear sky condition could be explained by the role of tree shade in UPF, while the lowest ΔPF with the greatest SZA and overcast cloud reveals the influence of overcast cloud cover and the increase in diffuse radiance with increasing SZA and (Table 10).

Diffuseness of UV and SZA

Although Fig. 2 is based on the Eq. (3) for in-shade exposure to UV, estimating overall exposure using Eq. (4) should also be calculated because UV radiation incident on the earth's surface is comprised of both a direct and a diffuse component. Just outside visible shade patterns of trees, UVB is reduced much more than PAR because more than half of the UVB irradiance arriving on earth is from diffuse radiation from the sky, whereas the sky fraction of the PAR is usually less than 0.25 with clear skies. Thus, where many large street-tree crowns block much of the sky, substantial protection from UVB is afforded for pedestrians, even in spots with direct visible sun (Heisler et al., 2003a,b).

This is why in-shade exposure differs considerably as canopy cover increases. A person in the shade of a tree has a UV reduction by that tree as well as by adjacent trees. Such an effect as stronger protection from grouped trees is more or less increased in our uniform tree spacing assumption. As canopy cover increases, adjacent trees at the same spacing become larger and more influential.

The combination of the diffuse and direct UV is termed global UV. The direct component is easier to minimize by simply blocking its path, as it is incident directly from the sun. However, the diffuse UV component is incident from all directions due to atmospheric and environmental scattering and can constitute a significant proportion of the UV exposure to the human body. The relative amounts of direct and diffuse UV compared to global UV depend on the SZA. The ratio of the diffuse UV to global UV increases with increasing SZA due to the longer path through the atmosphere (Parisi et al., 2010). For example, it seems to be noteworthy that the SZA was greatest, 28.64 degrees, when the lowest in-shade UPF in commercial and transportation land use occurred on August 31. This could be explained by the increase in diffuse fraction of above-canopy irradiance, which increases T_s with increasing solar zenith.

Other effects

In addition to canopy cover, cloud cover, and SZA, the variation of ΔPF might also be caused by differences in total column ozone, atmospheric aerosols, or building density. Absorption by aerosols under typical urban conditions reduces UV by 10–15%, although this can be substantially higher over heavily polluted sites (Fioletov et al., 2010). The algorithm for the TEMIS UVI data only implicitly contains the average aerosol load in De Bilt, Netherlands and Paramaribo, Suriname, ignoring the variations in aerosol by assuming typical values for the aerosol optical depth, which introduces an error of about 5% in the UVI (Allaart et al., 2004; van Geffen et al., 2005).

Conclusion

Trees contribute to reducing UV radiation to humans with results varying among land use types depending upon the amount of canopy cover. The model is built upon the equations from Grant et al. (2002) designed to forecast the reduced UV fraction at a below-canopy level in relation to above-canopy clear sky UV irradiance for varying cloud cover for in-shade and overall exposures. With the availability of input data such as UV, cloud cover, SZA and canopy cover by land use, this model should be applicable to other cities. Some of the necessary data were obtained from the i-Tree analysis for Seoul, and conversely, the model of this study is proposed to be included in the i-Tree program as a new component.

In the case of urban trees in Seoul, Korea in the summer of 2010, the average UPFs for the four months from May to August were estimated to be 8.3 for park and cemetery land use, 7.9 for vacant and agriculture, 3.4 for residential/multi-family, 3.2 for institutional, and 3.0 for commercial and transportation on the assumption that a pedestrian is in tree shade. The daily highest estimated UPF was 11.8. This occurred in the park and cemetery land use, which has the highest percent canopy cover, on May 20, when the sky condition was clear and the UVI value was 7.2. The lowest UPF was 1.7 in commercial and transportation land use, which has the lowest percent canopy cover, on August 31, when the cloud cover was overcast and the SZA greatest with the UVI of 2.6.

The unexamined factors in this study that usually influence UV radiation such as aerosol, and structures on the ground such as buildings will need to be considered for improving the model suggested here. For further research, comparison of UV protection by trees in different cities that already have i-Tree analyses could also be useful.

Acknowledgments

This work was funded by the USDA Forest Service, SUNY-ESF's Pack Institute Research Travel Award and New York State and Graduate Student Employees Union Professional Development Award. We thank Young Hee Sung and Berea World Mission for assistance with field data collection.

References

Allaart, M., van Weele, M., Fortuin, P., Kelder, H., 2004. An empirical model to predict the UV-index based on solar zenith angles and total ozone. Meteorol. Appl. 11, 59–65.

Bleasel, M.D., Aldous, S., 2008. In vitro evaluation of sun protection factors of sunscreen agents using a novel UV spectrophotometric technique. Int. J. Cosmet. Sci. 30, 259–270.

de Backer, H., Koepke, P., Bais, A., de Cabo, X., et al., 2001. Comparison of measured and modelled UV indices for the assessment of health risks. Meteorol. Appl. 8, 267–277.

CIE, 1987. A reference action spectrum for ultraviolet induced erythema in human skin. CIE J. 6, 17–22.

Diffey, B.L., Diffey, J.L., 2002. Sun protection with trees. Br. J. Dermatol. 147, 397–399.

Downs, N., Parisi, A., Turner, J., Turnbull, D., 2008. Modelling ultraviolet exposures in a school environment. Photochem. Photobiol. Sci. 7 (6), 700–710.

Fioletov, V., Kerr, J., Fergusson, A., 2010. The UV index: definition, distribution and factors affecting it. Can. J. Public Health 101 (4), I5–I9.

Gies, P., Elix, R., Lawry, D., Gardner, J., Hancock, T., Cockerell, S., Roy, C., Javorniczky, J., Henderson, S., 2007. Assessment of the UVR protection provided by different tree species. Photochem. Photobiol. 83, 1465–1470.

Grant, R., Heisler, G.M., Gao, W., 2002. Estimation of pedestrian level UV exposure under trees. Photochem. Photobiol. 75 (4), 369–376.

Grant, R., Heisler, G.M., Gao, W., Jenks, M., 2003. Ultraviolet leaf reflectance of common urban trees and the prediction of reflectance from leaf surface characteristics. Agric. For. Meteor. 120, 127–139.

Grant, R., Heisler, G.M., 2006. Effect of cloud cover on UVB exposure under tree canopies: will climate change affect UVB exposure? Photochem. Photobiol. 82 (2), 487–494.

Heisler, G.M., Grant, R.H., 2000. Ultraviolet radiation in urban ecosystems with consideration of effects on human health. Urban Ecosyst. 4, 193–229.

Heisler, G.M., Grant, R.H., Gao, W., 2002. Urban tree influences on ultraviolet irradiance. In: Slusser, J.R., Herman, J.R., Gao, W. (Eds.), Ultraviolet Ground and Space-based Measurements, Models, and Effects. Proceedings of SPIE. San Diego, CA.

Heisler, G.M., Grant, R.H., Gao, W., 2003a. Individual- and scattered-tree influences on ultraviolet irradiance. Agric. For. Meteorol. 120, 113–126.

Heisler, G.M., Grant, R.H., Nowak, D.J., Gao, W., Crane, D.E., Walton, J.T., 2003b. Inclusion of an ultraviolet radiation transfer component in an urban forest effects model for prediction tree influences in potential below-canopy exposure to UVB radiation. Proc. SPIE 5156, 228–235.

International Agency for Research on Cancer (IARC), 2012. IARC Monographs on the Evaluation of Carcinogenic Risks to Humans, Radiation: Volume 100D. World Health Organization.

Kim, J., Park, S.S., Cho, N., Kim, W., Cho, H.K., 2011. Recent variations of UV irradiance at Seoul 2004–2010 (서울의 최근 자외선 복사의 변화 2004–2010). Atmos. Korean Meteorol. Soc. 21 (4), 429–438, (written in Korean with English abstract).

Kinney, J.P., Long, C.S., Geller, A.C., 2000. The ultraviolet index: a useful tool. Dermatol. Online J. 6 (1), 2.

Lucas, R., 2010. Solar ultraviolet radiation: assessing the environmental burden of disease at national and local levels. In: Prüss-Ustün, A., Perkins van Deventer, E. (Eds.), Environmental Burden of Disease Series, No. 17. World Health Organization, Geneva.

McKinlay, A.F., Diffey, B.L., 1987. A reference action spectrum for ultraviolet induced erythema in human skin. CIE J. 6, 17–22.

National Toxicology Program (NTP), 2011. Report on Carcinogens, 12th ed. U.S. Department of Health and Human Services, Public Health Service, Research Triangle Park, NC, pp. 499pp.

Nowak, D.J., Crane, D.E., Stevens, J.C., Hoehn, R.E., Walton, J.T., Bond, J., 2008. A ground-based method of assessing urban forest structure and ecosystem services. Arboric. Urban For. 34 (6), 347–358.

Parisi, A.V., Kimlin, M., 1999. Comparison of the spectral biologically effective solar ultraviolet in adjacent tree shade and sun. Phys. Med. Biol. 44, 2071–2080.

Parisi, A.V., Turnbull, D.J., Schouten, P., Downs, N., Turner, J., 2010. Techniques for solar dosimetry in different environments. In: Gao, W., Schmoldt, D.L., Slusser, J.R. (Eds.), UV Radiation in Global Climate Change: Measurements, Modeling and Effects on Ecosystems. Tsinghua University Press, Beijing, pp. 192–204.

Parsons, P., Neale, R., Wolski, P., Green, A., 1998. The shady side of solar protection. Med. J. Aust. 168 (7), 327–330.

Qi, Y., Heisler, G.M., Gao, W., Vogelmann, T.C., Bai, S., 2010. Characteristics of UV-B radiation tolerance in broadleaf trees in southern USA. In: Gao, W.,

Schmoldt, D.L., Slusser, J.R. (Eds.), UV Radiation in Global Climate Change: Measurements, Modeling and Effects on Ecosystems. Tsinghua University Press, Beijing, pp. 509–530.
SCanning Imaging Absorption spectroMeter for Atmospheric CHartographY (SCIAMACHY). 2012. http://www.sciamachy.org/ (accessed November 2012).
US Environmental Protection Agency (EPA), 2010. Action steps for sun protection. http://www.epa.gov/sunwise/doc/actionsteps.pdf (accessed November 2012).
US EPA, 2012. How UV index is calculated. http://www.epa.gov/sunwise/uvicalc.html (last accessed November 2012).
US Department of Health and Human Services (HHS), 2012. National Health Observance Toolkit–July UV Safety Month. http://www.healthfinder.gov/nho/PDFs/JulyNHOtoolkit.pdf (accessed November 2012).
van Geffen, J., van der, A.R., van Weele, M., Allaart, M., Eskes, H., 2005. Surface UV radiation monitoring based on GOME and SCIAMACHY. In: Proceedings of the ENVISAT and ERS Symposium, Salzburg, Austria, SP-572, 6–10 September, 2004. ESA Publication.
Vanicek, K., Frei, T., Litynska, Z., Schmalwieser, A., 1999. UV-index for the public. In: A guide for publication and interpretation of solar UV Index forecasts for the public prepared by the Working Group 4 of the Cooperation in Science and Technology (COST)-713 Action UVB Forecasting COST-713 Action. Brussels.
World Health Organization (WHO), 1995. Protection against exposure to ultraviolet radiation. In: Rep. WHO/EHG/95. 17. World Health Organization, Geneva, Switzerland.
World Health Organization, 2002. Global Solar UV Index: A Practical Guide. A joint recommendation of the World Health Organization, World Meteorological Organization, United Nations Environment Programme, and the International Commission on Non-Ionizing Radiation Protection. World Health Organization, Geneva, Switzerland.
Yang, X., Miller, D.R., Montgomery, M.E., 1993. Vertical distributions of canopy foliage and biologically active radiation in a defoliated/refoliated hardwood forest. Agric. For. Meteorol. 67 (1–2), 129–146.
Yang, X., Heisler, G.M., Montgomery, M.E., Sullivan, J.H., Whereat, E.B., Miller, D.R., 1995. Radiative properties of hardwood leaves to ultraviolet irradiation. Int. J. Biometeorol. 38 (2), 60–66.
Yoshimura, H., Zhu, H., Wu, Y., Ma, R., 2010. Spectral properties of plant leaves pertaining to urban landscape design of broad-spectrum solar ultraviolet radiation reduction. Int. J. Biometeorol. 54 (2), 179–219.